The Saccade Main Sequence in Patients With Retinitis Pigmentosa and Advanced Age-Related Macular Degeneration

Leslie Guadron,[1] Samuel A. Titchener,[2,3] Carla J. Abbott,[4,5] Lauren N. Ayton,[4–6] John van Opstal,[7] Matthew A. Petoe,[2,3] and Jeroen Goossens[1]

[1]Department of Cognitive Neuroscience, Donders Institute for Brain, Cognition and Behaviour, Radboudumc, Nijmegen, The Netherlands
[2]Bionics Institute, East Melbourne, Victoria, Australia
[3]Medical Bionics Department, University of Melbourne, Melbourne, Victoria, Australia
[4]Centre for Eye Research Australia, Royal Victorian Eye & Ear Hospital, Melbourne, Victoria, Australia
[5]Department of Surgery (Ophthalmology), University of Melbourne, Melbourne, Victoria, Australia
[6]Department of Optometry and Vision Sciences, University of Melbourne, Melbourne, Victoria, Australia
[7]Department of Biophysics, Donders Institute for Brain Cognition and Behaviour, Radboud University, Nijmegen, The Netherlands

Correspondence: Jeroen Goossens, P.O. Box 9101, Nijmegen, HB 6500, The Netherlands; j.goossens@donders.ru.nl.

Received: October 12, 2022
Accepted: February 6, 2023
Published: March 1, 2023

Citation: Guadron L, Titchener SA, Abbott CJ, et al. The saccade main sequence in patients with retinitis pigmentosa and advanced age-related macular degeneration. *Invest Ophthalmol Vis Sci.* 2023;64(3):1. https://doi.org/10.1167/iovs.64.3.1

Purpose. Most eye-movement studies in patients with visual field defects have examined the strategies that patients use while exploring a visual scene, but they have not investigated saccade kinematics. In healthy vision, saccade trajectories follow the remarkably stereotyped "main sequence": saccade duration increases linearly with saccade amplitude; peak velocity also increases linearly for small amplitudes, but approaches a saturation limit for large amplitudes. Recent theories propose that these relationships reflect the brain's attempt to optimize vision when planning eye movements. Therefore, in patients with bilateral retinal damage, saccadic behavior might differ to optimize vision under the constraints imposed by the visual field defects.

Methods. We compared saccadic behavior of patients with central vision loss, due to age-related macular degeneration (AMD), and patients with peripheral vision loss, due to retinitis pigmentosa (RP), to that of controls with normal vision (NV) using a horizontal saccade task.

Results. Both patient groups demonstrated deficits in saccade reaction times and target localization behavior, as well as altered saccade kinematics. Saccades were generally slower and the shape of the velocity profiles were often atypical, especially in the patients with RP. In the patients with AMD, the changes were far less dramatic. For both groups, saccade kinematics were affected most when the target was in the subjects' blind field.

Conclusions. We conclude that defects of the central and peripheral retina have distinct effects on the saccade main sequence, and that visual inputs play an important role in planning the kinematics of a saccade.

Keywords: eye movements, saccade kinematics, optimal control, tunnel vision, central vision loss

Saccades are rapid movements of the eye that direct the fovea to different parts of the visual field as quickly and as accurately as possible. They range in amplitude from the small movements made while scrutinizing details in a picture, for instance, to the much larger movements made while gazing around at the surrounding scenery. In healthy vision, both the fovea and the peripheral retina play critical roles in gathering information from the environment. The fovea supports high-acuity central vision and provides the origin of the oculomotor reference system for saccadic eye movements. The peripheral retina provides side (peripheral) vision and is important for scotopic vision, spatial navigation, motion detection, and saccadic orienting behavior.

Normal saccades can be characterized by a set of stereotypical relationships among saccade amplitude, duration, and peak velocity, known as the main sequence.[1] These relationships are reliably replicated among healthy humans (see Refs. 2 and 3, for review): the duration and peak velocity increase as the amplitude of the saccades increases. Particularly, the increase is linear for small saccades, whereas the peak velocity shows a saturating nonlinearity for large saccades. This highly stereotyped behavior has been hypothesized to reflect an optimization process that the brain carries out when planning eye movements to optimize vision in the presence of internal noise and peripheral visual uncertainty.[4–7]

The main sequence has been used to characterize eye-movement dysfunction in a range of patients, including patients with palsy of the extra-ocular muscles, myasthenia gravis, cerebellar disorder, ocular progressive supranuclear palsy, multiple sclerosis, spino-cerebellar and cerebellar ataxia, and Parkinson's disease (for review, see Ref. 2). By contrast, little is known about how retinal diseases and vision loss might influence the main sequence. Saccades are said to be ballistic because they usually do not last long enough to be influenced by visual feedback. Even so, patients with retinal damage will have a visual input that differs from that of those with healthy vision. This in turn may cause altered saccadic behavior when optimizing vision under the constraints imposed by the patient's visual impairment.

In healthy vision, the brain should minimize saccade duration to limit the amount of time during which vision is poor due to image blur and saccadic suppression.[8] But, to move the eye very quickly, a strong control signal to the (sluggish) muscles is needed. Physiological recordings have indicated, however, that these neural signals are perturbed by multiplicative noise, by which the level of noise increases with increasing activation levels.[9–12] Thus, moving the eye more quickly induces more noise in the control signals, and hence leads to increased end point variability. Moreover, spatial resolution in the retinal periphery is considerably lower than in the fovea, which introduces additional uncertainty about target locations. Therefore, for optimal performance, the brain needs to optimize the control signals in a way that minimizes saccadic duration while maintaining sufficient accuracy.[4] The main sequence relationships between saccade duration and velocity are believed to achieve this balance.[4,13–15]

To test this theory in normally sighted subjects, we recently manipulated the accuracy constraints of a pro-saccade task by varying the size of the visual saccade targets.[16] We reasoned that to meet the increased precision demands for the smallest targets, saccades to those targets would have to be slower than the ones to the largest targets in order to reduce the detrimental effects of the velocity-dependent motor noise on the end point accuracy. Interestingly, we found that saccades to the smallest targets were indeed more accurate and typically slower than amplitude-matched saccades to the larger targets, but other factors, such as saccade latency, influenced the main sequence as well.

In subjects with reduced vision, the optimal trade-off between accuracy and speed might also differ. For instance, if high-resolution vision in the fovea is lost, as is the case in subjects with age-related macular degeneration (AMD),[17] saccade accuracy might be less important than in normal vision. In this case, subjects could afford to make faster but less accurate saccades. In patients with glaucoma or retinitis pigmentosa (RP), who suffer from tunnel vision, the loss of peripheral vision might lead to a high level of uncertainty about the target location, which could in turn affect motor commands. Recent findings indeed show that saccade peak velocity correlates with statistical decision confidence[18] as they do with target size.[16]

Although the nature of the change in kinematics is perhaps difficult to predict, examining the saccades of patients with different retinal lesions could provide further insight into the role of vision in saccade planning and execution, as well as a better understanding of the visuomotor system. We therefore set out to study patients who acquired vision loss as a result of either AMD or RP. AMD causes a loss of central vision due to photoreceptor cell and retinal pigment epithelial damage in the macula, the part of the eye with the highest density of visual receptors. RP, or rod-cone dystrophy, causes a loss of peripheral vision due to the primary degeneration of the rod photoreceptor cells, which have their highest density outside of the macula. In both diseases, vision loss is gradual and scotomas (blind spots) develop and grow over time.

Patients with AMD may compensate for their foveal vision loss by developing what is known as a preferred retinal locus (PRL) or eccentric fixation, which is a "new fovea" that is used by the patients for fixation and for acquiring saccade targets (see, for example, Ref. 17, for a comprehensive review). Not all patients with AMD develop a PRL. It is an adaptation predominantly seen in those who have lost binocular foveal vision. Patients who still have vision in one fovea will tend to continue using their natural fovea for fixation.[17,19] The stability of fixation with the PRL varies, although there is typically some level of impairment, and it is not necessarily related to the distance of the PRL from the fovea.[20] This can improve over time, however, and patients who have used a PRL for years may develop oculomotor behaviors that approximate those of people with healthy vision.[21]

Many studies have investigated eye movements in patients with visual deficits and in healthy subjects with simulated deficits. This was typically accomplished with a visual search task and the main outcome measures included saccade amplitude, fixation duration, time to complete task, and number of saccades needed to complete the task.[22–24] Typically, in patients with AMD, search times increase and the number of saccades needed to find the target also increase compared to healthy controls. Patients with AMD also had longer inter-saccade intervals and made saccades with smaller amplitudes.[24] Patients with RP, on the other hand, displayed behavior similar to that of controls with normal visual fields. In a visual search task, their search duration, fixation duration, saccade size, and number of saccades did not differ significantly from controls.[25] Another study where subjects freely made saccades while walking confirmed that the direction and amplitude of saccades made by patients with RP were comparable to those of control subjects.[26] However, a more recent study found that patients with RP tend to move their heads more and their eyes less than normally sighted subjects during a visual search task.[27] Although these studies investigated the search strategy of patients, and compared them to healthy subjects, they did not study the properties of the saccades themselves.

Two studies have reported the main sequence of patients with vision loss. One was carried out in patients with tunnel vision[26] and the other in patients with central vision loss.[28] The former study (which used a visual search task) did not find any differences between the main sequence of patients and that of healthy subjects. However, they did not measure the control data themselves and arrived at this conclusion by comparing their patients' saccades to previously published data from healthy subjects. The latter study reported that saccades in patients with long-standing maculopathies had lower peak velocities and longer durations compared to that of healthy subjects.[28] An analysis of the saccade kinematics in patients with vision loss is rare and, as far as we know, has not been presented elsewhere. Our study is of value given that we tested patients with different visual deficits and healthy controls on the same task. This enabled us

to directly compare the main-sequence properties of these different groups.

We hypothesized that due to the different compensation strategies used by the patients with loss of foveal vision and those that are suffering from a selective loss of their peripheral vision, we would see differences between the main sequence of patients with RP and patients with AMD and that of healthy subjects.

Methods

Participants

We recruited five patients with moderately advanced RP, six patients with bilateral geographic atrophy due to late atrophic AMD, and seven healthy control subjects with normal vision (NV). The patients with RP we selected were required to have some remaining central vision in each eye. Central visual acuity in these patients was between 20/400 and 20/32 (see Table 1). Adhering to the Beckman classification,[29] the patients with AMD had to be 50 years or older with bilateral geographic atrophy. Their monocular visual acuities ranged between 20/32 and 20/800 (see Table 1). Controls (NV) had no eye disease, nor cause for reduced visual acuity, and had a normal or corrected to normal visual acuity of 20/25 or better in either eye.

Exclusion criteria for all three subgroups were (i) any diagnosis of neuro-muscular disorder likely to affect oculomotor control (i.e. previous stroke, Parkinson's disease, muscular dystrophy, or multiple sclerosis), and (ii) pathological nystagmus. Their ages ranged from 41 to 84 years old (see Table 1), however, all patients with AMD were 50 years or older, by definition.

The subjects gave informed consent in writing and had an ophthalmologic examination, including Goldmann perimetry (size V and III target) or Macular Integrity Assessment (MAIA; CentreVue) to assess the visual field, and multimodal imaging including non-dilated color fundus photography (CFP; Canon CR6-5NM non-mydriatic camera, Japan), near infrared (NIR; Heidelberg Spectralis, Germany), and optical coherence tomography (OCT; Heidelberg Spectralis, Germany) imaging. Behavioral eye movement data were collected following ocular examination, with a break of at

Table 1. Participant Characteristics

Subject ID	Diagnosis	Age (Years)	Sex	Visual Acuity (Snellen)	PRL Eccentricity (Degrees)	Fixation Stability (deg^2)
1	AMD	68	M	OD 20/32	OD 7.7	OD 4.0
				OS 20/800	OS 4.6	OS 7.5
2	AMD	84	F	OD 20/100	OD 6.9	OD 4.8
				OS 20/40	OS 8.2	OS 6.1
3	AMD	68	F	OD 20/80	OD 10.8	OD 18.7
				OS 20/200	OS 10.5	OS 19.3
4	AMD	76	F	OD 20/100	OD 2.2	OD 0.5
				OS 20/160	OS 3.5	OS 1.1
5	AMD	70	M	OD 20/200	OD 3.3	OD 5.4
				OS 20/50	OS 5.4	OS 1.3
6*	AMD	84	F	OD 20/50	OD 0.0	OD 4.2
				OS 20/20	OS 0.0	OS 0.1
7	RP	41	F	OD 20/32		
				OS 20/63		
8	RP	52	M	OD 20/80		
				OS 20/250		
9	RP	70	F	OD 20/100		
				OS 20/400		
10	RP	77	M	OD 20/32		
				OS 20/32		
11	RP	71	M	OD 20/40		
				OS 20/160		
12	NV	44	F	OD 20/16		
				OS 20/16		
13	NV	73	M	OD 20/16		
				OS 20/16		
14	NV	71	M	OD 20/20		
				OS 20/20		
15	NV	67	F	OD 20/20		
				OS 20/20		
16	NV	60	F	OD 20/10		
				OS 20/10		
17	NV	74	M	OD 20/16		
				OS 20/20		
18	NV	50	M	OD 20/20		
				OS 20/20		

Patients diagnosed with age-related macular degeneration (AMD, $n = 6$) or retinitis pigmentosa (RP, $n = 5$) were included as well as normally sighted controls (NV, $n = 7$). Listed are the subjects' age and sex (F: female, M: male), the patients' monocular visual acuities, and for the patients with AMD, the PRL eccentricities and fixation stability (63% bivariate contour ellipse area).

* S6 had normal central acuity in her left eye, and this eye was occluded for eye movement testing.

Investigative Ophthalmology & Visual Science

least 15 minutes to ensure no ongoing aftereffects from the imaging.

The study was reviewed and approved by the human research ethics committees of the Royal Victorian Eye and Ear Hospital and the Bionics Institute, and conducted in accordance with the Declaration of Helsinki, with all participants providing informed consent.

Setup

Participants were seated 60 cm in front of a 30-inch computer screen (Dell U3011, 2560 × 1600 pixels) in an otherwise dark, soundproof room. The position of both eyes was measured with a remote eye-tracking system (Eyelink 1000 Plus, SR Research) at a sampling rate of 500 Hz per eye. Subjects were asked to keep their head still during the measurements with the help of a chin rest. A target sticker on the forehead ensured steady tracking even when small head movements occurred. The stimulus software was written in Matlab (version 2014) using the Psychophysics Toolbox extension[30] and executed on a laptop computer equipped with an open GL graphics card.

A 13-point calibration of the eye tracker was carried out prior to each measurement. The calibration targets were filled white circles with a diameter of 1 degree against a black background. We ensured that each eye was calibrated individually while the other eye was covered. This monocular viewing forced the participants to use the PRL of that eye during fixation of the calibration targets. NV controls and patients with RP all had foveal PRLs. All but one patient with AMD had peripheral PRLs, located using the MAIA microperimetry records. The most eccentric calibration points were sometimes not visible to the subjects with RP because of their limited peripheral vision. In these cases, the experimenter verbally directed the subject to the location of the calibration target or audibly tapped on the screen to help them find it.

Task

Subjects performed a horizontal center-out saccade task. Every trial started with a tone and the presentation of a fixation point at the center of the screen. The participant was instructed to fixate on the fixation point for as long as it was present. The fixation period varied pseudo-randomly from trial to trial (range = 800–1800 ms). As soon as the fixation point disappeared, a target appeared along the central horizontal axis of the screen, either to the right or to the left of the fixation point. Subjects were asked to make a rapid eye movement to the target and to press a button once they had acquired the target. The target remained on the screen until the button was pressed or until 10 seconds had passed. The inter-trial interval was 500 ms.

The target and fixation point were both filled white circles with a diameter of 1 degree against a black background. The target location was pseudo-randomly chosen on every odd trial. In every subsequent even trial, the target was presented at the same location as in the preceding odd trial. There were 16 possible target locations: 2, 5, 9, 12, 16, 20, 22, and 25 degrees to the right and to the left of the central fixation point. Subjects were informed that each target was presented at the same location twice in a row. On the second presentation, in the even trials, the fixation point was changed to a white circle with a black triangle inscribed inside of it. The triangle pointed to the side of the screen on which the target would appear. This was meant to aid the patients with RP who may not have been able to see the target the first time it was presented and had to search for it. We hoped that on the second presentation they would be able to make a single saccade to the target.

Subjects completed 4 blocks, each consisting of 128 trials with 4 repetitions per condition. Each block took about 5 minutes to complete. Subjects could take a short break after every block. In one of the patients with AMD (S6), we blocked vision of the left eye after the first block of trials because she had no central vision loss in that eye. This blocking was done with an infra-red transparent filter so movements of the covered left eye could still be recorded.

Data Analysis

The offline analysis was performed in Matlab (version 2020a). In all analyses, we used head-referenced eye position signals (in degrees) that were filtered offline, first with a 5-point median filter and then by a 16th order low-pass Butterworth filter with an 80 Hz cutoff frequency and zero phase delay.

Saccade Detection. Saccades were marked with custom software using separate velocity and acceleration criteria for movement onsets (40 deg/s and 7500 deg/s^2) and offsets (30 deg/s and −5000 deg/s^2). Eye velocity was computed from the vector sum of the horizontal and vertical eye-velocity components. Eye acceleration was the time derivative of this track eye-velocity signal. Post saccadic oscillations (PSOs), likely reflecting relative movements between the pupil and the iris rather than eyeball oscillations,[31] were discarded. This was done by including a direction-reversal criterion. More specifically, the algorithm detected points where the direction of the instantaneous eye-velocity vector first changed more than 120 degrees compared with the initial direction of the saccade up until its peak velocity. Movements of the left and right eyes were marked independently. All onset and offset markings were visually inspected and corrected if deemed necessary. Movements with blink artifacts were discarded.

Saccade Parameters. Saccade latency was the time difference between target onset and movement onset. Saccade duration was the time difference between the saccade onset and offset markers, discarding any PSO as described above. Saccade amplitude was taken as the vectorial eye displacement during this interval. Peak velocity was defined as the maximum vectorial eye velocity that occurred during a saccade. To suppress noise in this measure, the horizontal and vertical eye velocity signals computed from the head-referenced eye position signals were low-pass filtered at 40 Hz with a zero phase, eighth order Butterworth filter (as recommended by Ref. 32). This filtering at 40 Hz, instead of at 80 Hz, was only applied to determine peak velocity.

We noticed that some of the patients made many saccades with double or multi-peaked velocity profiles. To dissociate these saccades systematically from saccades with single-peaked velocity profiles, we used a peak finding routine (findpeaks) with the minimum peak prominence set to 4 times the root mean square (RMS) value of the velocity noise and counted all velocity peaks with a prominence greater than 30% of their height. The RMS level of the velocity noise was determined from a 100 ms fixation period just before saccade onset.

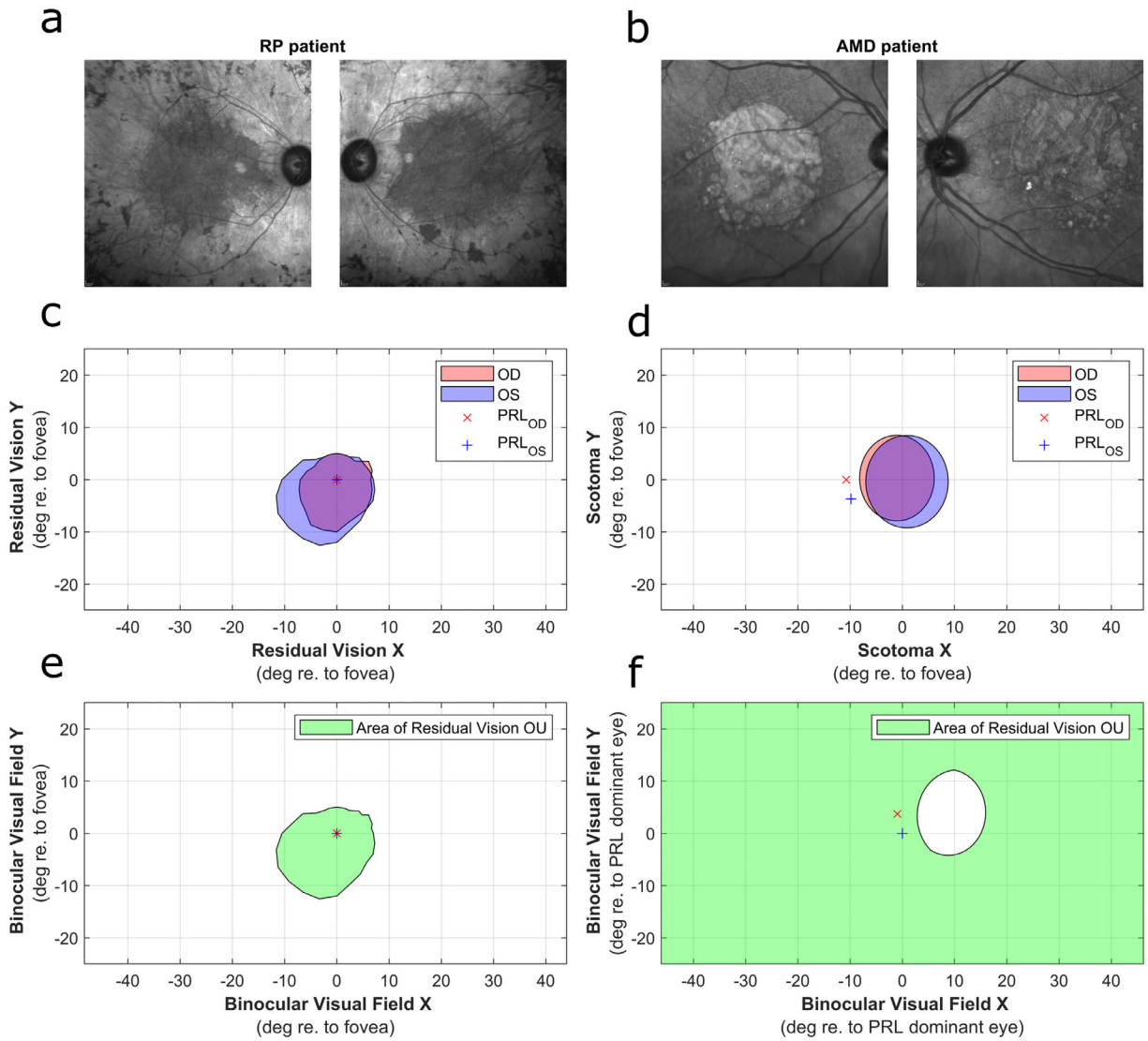

Figure 1. Visual field estimation. (**a, b**) Near infrared images from a patient with RP (S10; **a**) and a patient with AMD (S3; **b**) showing their retinal lesions in the right and left eyes. (**c, d**) The areas of residual vision in each of the two eyes of a patient with RP as inferred from Goldmann perimetry **c** and the location of scotomas in a patient with AMD as inferred from multi-modal imaging **d**. The PRL for monocular viewing with the right eye (OD; *red x*) and left eye (OS; *blue* +) was estimated with MAIA. (**e, f**) Area of residual binocular vision relative to the fovea (patient with RP; assuming both eyes foveate the same point) or relative to the PRL of the dominant eye (patient with AMD; assuming alignment of the foveal axes).

To evaluate the saccade end point accuracy, we computed the retinal coordinates of the target at movement onset and offset in each of the two eyes (target location relative to the eye minus eye position). As a consequence of the applied calibration procedure, retinal target eccentricity was expressed relative to the fovea (subjects with NV or RP) or the eye's PRL (subjects with AMD).

Visual Field Estimation. As is illustrated in Figures 1c and 1d, the areas of residual vision in each of the two eyes were estimated from Goldmann perimetry (patients with RP; Fig. 1a) or MAIA microperimetry results (patients with AMD; Fig. 1b) and expressed as two-dimensional polygons. The data from these functional tests was correlated with anatomic retinal measures from multimodal imaging. More specifically, in patients with AMD, fundus autofluorescence (FAF) was used to identify the scotoma area, OCT was used to identify the fovea, MAIA was used to identify the PRL, and NIR was used to co-register all that in a single image. The coordinates of the PRL relative to the fovea were derived from the most stable point of fixation during MAIA testing. The foveal position was determined directly from the cross-sectional OCT B-scan images showing the precise foveal pit position relative to the matching en face NIR image seen with the Heidelberg Spectralis OCT. The en face NIR image was mapped directly to the MAIA NIR image using the blood vessel pattern to compare foveal position with the PRL. MAIA was only performed for the purpose of measuring fixation; visual sensitivity thresholds were not assessed.

As the monocular calibration procedure ensured that the eye movement data from the left and right eye provided either the coordinates of the fovea (NV controls and patients with RP) or PRL (patients with AMD) of the recorded eye, this allowed us to determine the location of the residual

Investigative Ophthalmology & Visual Science

visual field of each eye on a sample-to-sample basis. The residual visual fields were then combined to determine the binocular residual field, that is, the area in which a stimulus would fall on an intact part of the retina in at least one of the two eyes given the current eye positions. Figures 1e and 1f illustrate the resulting binocular residual field for a patient with RP and a patient with AMD, both under the assumption that the foveal axis of the two eyes align. In cases where the eye position signal from one eye was transiently lost, the location of the affected field of that eye was estimated from the position of the other eye under the same assumption.

Using these visual field estimates, we determined for each saccade onset if the target fell within the affected visual field of both eyes or not. In addition, we determined if the saccade vector itself ended at a location within the binocular residual field or not.

Data Selection. Data were separated into odd trials, that is, trials in which the target appeared at unpredictable locations, and even trials, that is, trials in which the participants could predict the target location from the previous trial and in which the cuing triangle was inscribed in the fixation point. In addition, we selected saccades based on their timing within the trial and/or endpoint. Primary saccades were the first saccades in a trial that occurred at least 80 ms after the target appeared and that were directed away from the fixation point. The latter ensured that we excluded saccades aimed at refixating the fixation point. We also identified the largest goal-directed saccade in each trial. These were saccades that occurred at least 80 ms after the target appeared and that brought the target closest to the fovea/PRL. In part of the analyses, we further discriminated between saccades with single-peaked velocity profiles and multi-peaked velocity profiles.

Statistics. We used the Matlab Statistics and Machine Learning Toolbox (version 2020a) for statistical evaluation of the results. Parametric and non-parametric tests were applied to compare groups as indicated in the text. Unless otherwise indicated, all tests were two-sided and P values less than 0.05 (type I error) were considered statistically significant.

The evaluation of the saccade kinematics had to account for the systematic increase in saccade duration and peak velocity as a function of saccade amplitude. To accomplish this, we compared saccades of subjects with RP and AMD to amplitude matched saccades of controls with NV in 2-degree-wide amplitude bins (except for the 1-degree amplitude bin for which the width was reduced to 1 degree). For each subject and each amplitude bin, we determined the median duration and median peak velocity of saccades recorded for leftward and rightward saccades and for each of the two eyes, and we made boxplots of the grouped data to visualize the results. We applied bin-wise comparisons between the patient groups and NV control group using non-parametric Wilcoxon rank sum tests. However, this parsimonious comparison did not account for the nested structure of the data and involved repeated testing. To address these shortcomings, we analyzed the main sequence relationships further using mixed effects regression. In this analysis, we assumed an affine relationship between saccade amplitude, R (in degrees), and saccade duration, D (in ms):

$$D = a \times R + b \quad (1)$$

with constants a (in ms/deg) and b (in ms). In addition, we assumed a nonlinear relation between saccade amplitude and saccade peak velocity, Vp (in deg/s):

$$Vp = 1/(\alpha/R + \beta) \quad (2)$$

Vp saturates for $R \to \infty$ with a value $Vp_{max} = 1/\beta$ (in deg/s) and decreases for $R \to 0$ with a slope of $1/\alpha$ (in s^{-1}). Note that Equation 2 can be rewritten as an affine relation between $1/R$ (in deg^{-1}) and $1/Vp$ (in s/deg):

$$1/Vp = \alpha \times 1/R + \beta \quad (3)$$

which simplifies the fit procedure to general linear modeling with a reciprocal link function.

The fixed effects in the regression analyses were saccade amplitude and participant group (NV, RP, and AMD). We used either mixed-effects linear regression (using fitlme) or general linear modeling with a reciprocal link function (using fitglme) to estimate the fixed effects on saccade duration and peak velocity, respectively. In both cases, we allowed for random effects on the intercepts and slopes to accommodate intersubject variability. The random effects were grouped by subject, by movement direction within subject, and by recorded eye within movement direction to account for the nested structure of the repeated measurements.

Results

Figure 2 illustrates the horizontal center-out saccade task that the subjects performed. Plotted are the horizontal eye-in-head position of the right (red) and left (blue) eye as a function of time for a subject with NV, a subject with RP, and a subject with AMD. Each panel shows two responses towards the same target, both occurring in an odd trial, that is, when the target appeared at an unpredictable, pseudo-randomly selected location (Methods). As indicated by the dashed lines, the targets appeared at either 9 or 22 degrees to the right of the central fixation point (see Figs. 2a–c and Figs. 2d–f, respectively). The targets at 9 degrees to the right were in the intact visual field of the patient with RP but in the impaired visual field of the patient with AMD. Conversely, the targets at 22 degrees to the right were in the intact visual field of the patient with AMD, but in the impaired visual field of the patient with RP. A target was considered in the intact visual field of the subject if it appeared in the area of residual vision of at least one eye (Methods). The areas of residual vision for the two patients in Figure 2 are plotted in Figure 1.

Note the non-zero eye positions during the initial fixation period. This is because fixation of a point on the screen with both eyes required approximately 6 degree vergence. Furthermore, in both patients, targets that appeared in the intact visual field evoked a single, goal-directed saccade followed by a smaller corrective saccade, a response pattern also seen in the subject with NV. For targets in the impaired visual field, the response pattern differed, especially in the patient with RP. In this patient, either the response was broken up into two or more saccades in the correct direction, or the initial saccades were in the wrong direction and then the subject made a series of saccades in the opposite direction while searching for the target. Similar response patterns were observed in the other patients with RP when they had to guess about the target's location in their impaired visual field. The traces also illustrate the occurrence of markedly large PSOs in patients with RP. In the present study, we have

Investigative Ophthalmology & Visual Science

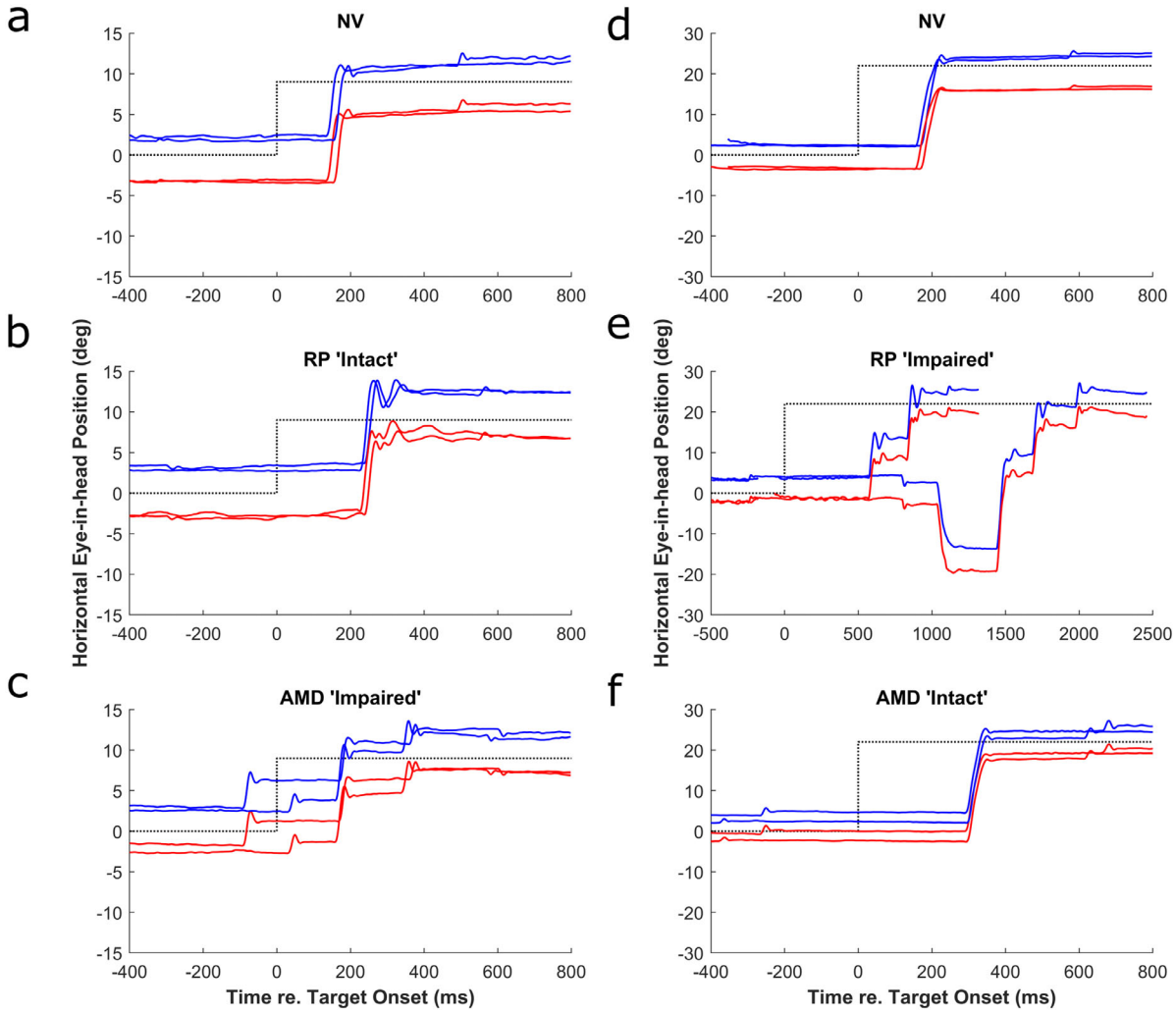

Figure 2. Example traces. Horizontal movements of the left (*blue*) and right (*red*) eye of single participants with NV, RP, and AMD (S15, S10, and S3, respectively). Each plot shows two trials with responses to the same stimulus. *Dashed lines* indicate the stimulus locations relative the cyclopean eye. Targets appeared at 9 degrees (**a, b, c**) or 22 degrees (**d, e, f**) to the right of the central fixation point. For the patients, either the targets at 22 degrees (patient with RP) or the targets at 9 degrees to the right (patient with AMD) were in their impaired visual field just prior to the first saccade. Data are from odd trials with targets at unpredictable, pseudo-random locations. Note scaling differences between the panels.

discarded the PSOs from our analyses (Methods), but we will quantify them in more detail in a separate study.

Saccade End Points

Figures 3a to 3c show the accuracy of the subjects' primary saccades by plotting the saccade amplitude as a function of the target eccentricity (relative to the fovea or the PRL) at saccade onset. Positive and negative values denote targets or saccades in the right and left visual fields, respectively. Perfectly accurate responses fall on the diagonal line. Data are from the same individuals as in Figure 2, and are from odd trials only (i.e. when the target appeared at an unpredictable location). Black data points denote the responses to targets that were in the patients' impaired visual field at the beginning of the movement. Apart from a limited number of misdirected saccades, the subject with NV and the subject with AMD made accurate responses. The subject with RP, on the other hand, was only accurate for stimuli presented in his intact visual field (red points). For targets in his impaired visual field (black points), there was hardly any correlation between saccade amplitude and target eccentricity, indicating that this participant merely guessed where the target had appeared. By comparison, the accuracy of the subject with AMD for targets within her scotoma (black) was clearly better. Supplementary Figure S1 shows the accuracy of primary saccades in all individual subjects.

The boxplots in Figures 3d to 3f, quantify the Spearman rank correlations between saccade amplitude and retinal target eccentricity in each of the three groups. Figure 3d shows the results for all target locations combined, whereas Figures 3e and 3f are for targets that appeared in the patients' intact or impaired visual field, respectively. Note that considering all odd-trial responses, the correlations between saccade amplitude and target eccentricity were very weak for patients with RP (RP: median $\rho = 0.10$; range = 0.06–0.16). In patients with AMD, these correlations were stronger (AMD: median $\rho = 0.91$; range = 0.88–0.97), but still significantly weaker (Wilcoxon rank sum test: $P < 0.005$) than in the control group (NV: median $\rho = 0.986$;

Investigative Ophthalmology & Visual Science

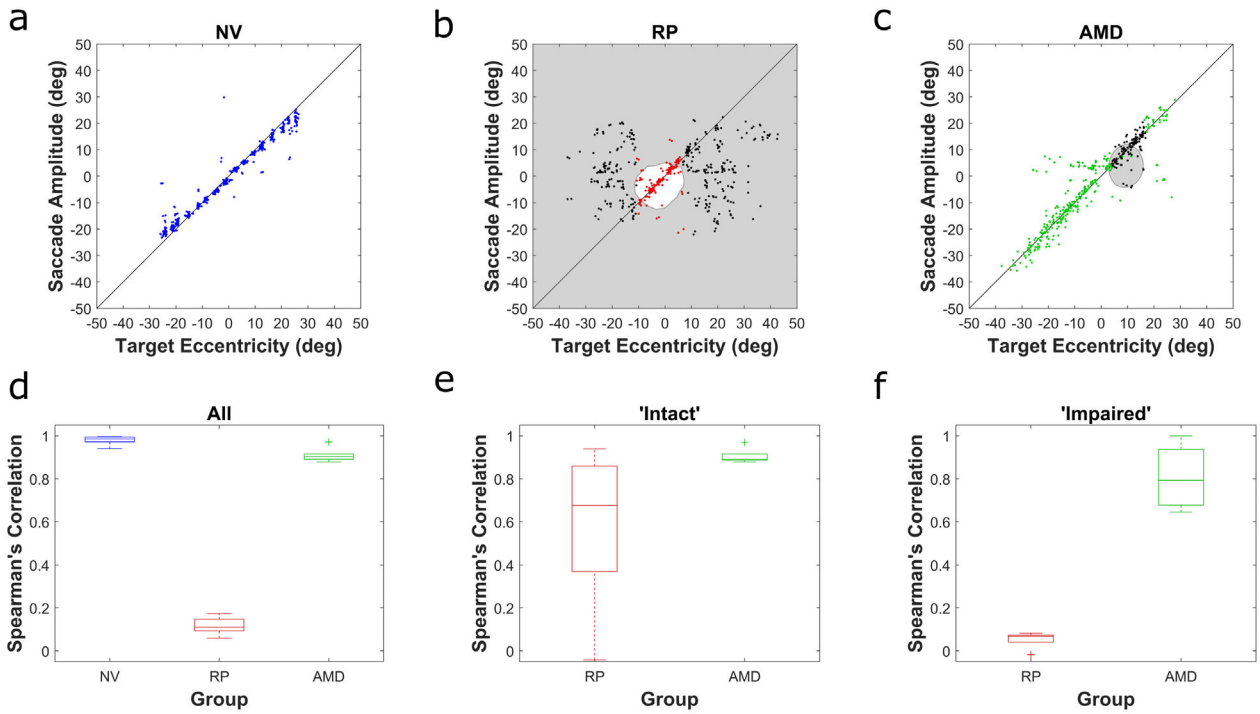

Figure 3. End points primary saccades. (**a, b, c**) Single subject data from participants with NV, RP, and AMD (same three participants as in Fig. 2). Saccade amplitude as a function of target eccentricity relative to the fovea or the PRL just before saccade onset. Positive eccentricities/amplitudes are for targets/movements to the right; negative eccentricities/amplitudes are for targets/movements to the left. Data are pooled across left and right eyes. *Insets* illustrate the two-dimensional visual field defects, with the *gray* area representing impaired sensitivity in both eyes. *Black dots*: Target was in the impaired visual field of both eyes at movement onset. *Colored dots*: Target was in the intact visual field of at least one of the two eyes. (**d, e, f**) Boxplots showing Spearman's rank correlations between target eccentricity and saccade amplitude in each group. On each box, the central mark indicates the median, and the bottom and top edges of the box indicate the 25th and 75th percentiles, respectively. The whiskers extend to the most extreme data points not considered outliers, and the outliers (defined as any value that is more than 1.5 times the interquartile range away from the bottom or top of the box) are plotted individually using the "+" symbol.

range = 0.950–0.996). Considering only the saccades in either the intact or impaired visual field, the correlations between saccade amplitude and target eccentricity were significantly worse for the patients with RP compared with patients with AMD (Wilcoxon rank sum tests: $P < 0.05$ and $P < 0.01$, respectively). In fact, for patients with AMD, the localization of targets within their impaired visual field was surprisingly good (median $\rho = 0.79$; range = 0.56–0.99). The sizes and location of their scotomas might explain this relatively good performance of the AMD group to some extent.

Figure 4 shows the visual field impairments of the right (OD) and left (OS) eye and for the two eyes combined (OU) in all tested patients with RP (see Fig. 4a, residual field) and patients with AMD (see Fig. 4b, scotomas). Each color represents a different subject. Note, in Figure 4a, that all patients with RP had extensive loss of peripheral vision on the horizontal meridian of both eyes. As a result, many of the stimuli fell in the impaired visual field of both eyes. In the patients with AMD, however, vision loss was restricted to their scotomas (see Fig. 4b), the location of which differed between the two eyes, and did not always encompass the horizontal meridian. In S1 (AMD, dark blue), for instance, the overlapping parts of the scotomas in his left and right eye were above the PRL of his dominant (right) eye. As a result, the target only had a chance of falling within the impaired visual field of both eyes when the participant incidentally deviated his gaze down from the fixation point. In S2 (AMD, red) there was no overlap between the scotomas in her left and right eye for the eye positions assumed in the right-hand plot and in S4 (AMD, pink), the overlap was very small. Consequently, for these subjects too, there were very few trials with the target appearing exclusively in both scotomas. Last, in S6 (AMD, cyan), two of the three large scotomas in her right eye as well as the one surrounding the fovea of the left eye encompassed the horizontal meridian. However, their overlap was small, and because Goldmann perimetry indicated no loss of sensitivity in her left eye, we blocked vision of her left eye with an infra-red transparent filter for most of the trials (Methods).

Figure 5 examines the end points of the largest goal-directed saccades in the odd trials using the same format as Figure 3. Oftentimes, these goal-directed saccades were primary saccades except in subjects with RP. As illustrated by the traces in Figure 2, and reported in previous studies with patients with RP,[33] these subjects had to search for the target if it appeared in their peripheral visual field. Following one or more saccades in the wrong direction, the subject would then make one or more large saccades in the opposite direction. In effect, we found that in patients with RP, the amplitudes of the largest goal-directed saccades correlated much more strongly with target eccentricity measured at the beginning of those saccades (RP: median $\rho = 0.91$; range = 0.57–0.98) than was observed for primary saccades. The scatter plot in Figure 5b, with data from the same patient with RP as in Figure 3, readily illustrates the occurrence of very

Investigative Ophthalmology & Visual Science

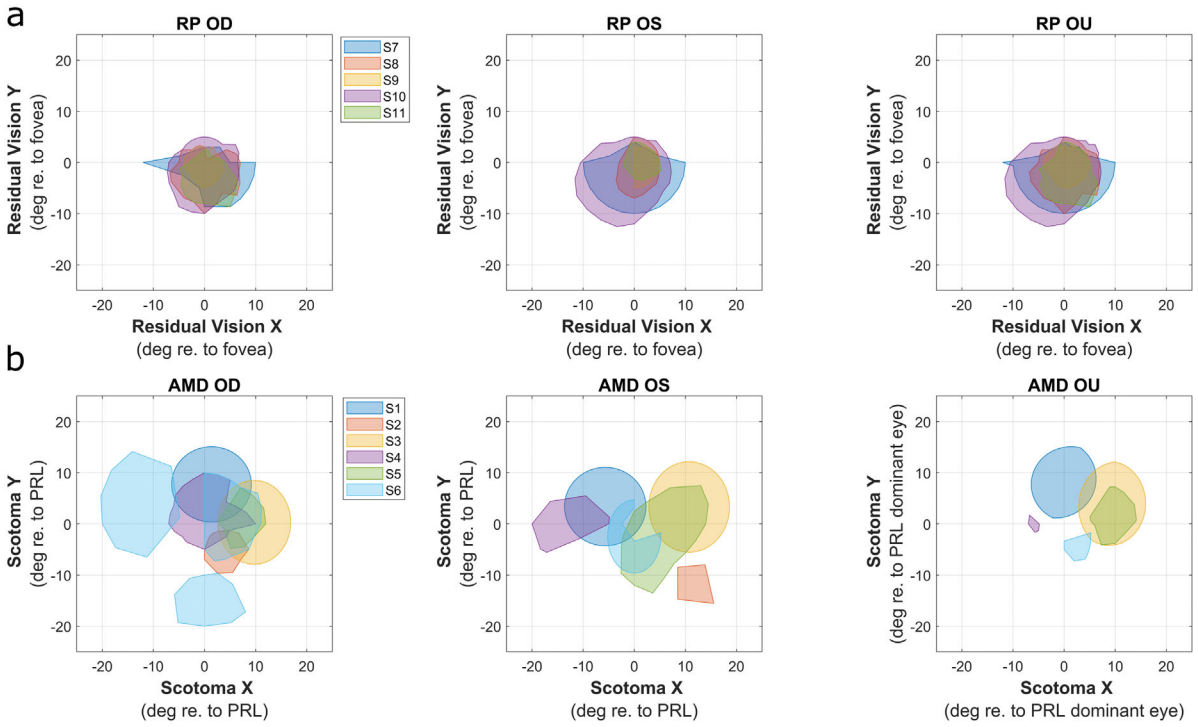

Figure 4. Residual visual fields and scotomas. (**a**) Area of residual visual field in the right (OD) and left (OS) eye relative to the fovea (and measured eye position) in all five participants with RP. (**b**) Location of scotomas in the right and left eye relative to the PRL of the corresponding eye (and measured eye position) in all six participants with AMD. Areas of residual vision (RP) or vision loss (AMD) for the two eyes combined were estimated from the monocular fields and the measured position of the eyes on a sample-to-sample basis. Here, we show them, for illustration purposes, relative to the PRL of the dominant eye assuming that both foveas are directed toward the same point in space.

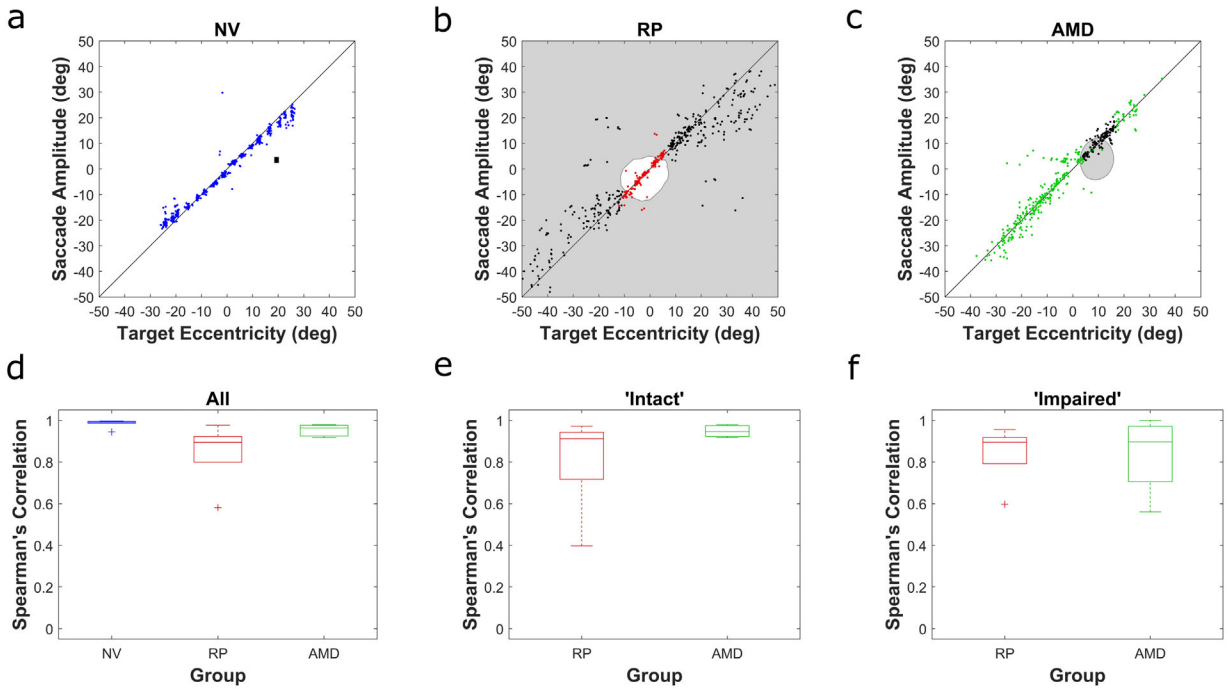

Figure 5. End points largest goal-directed saccades. (**a, b, c**) Single subject data. (d, e, f) Box plots showing Spearman's rank correlations between saccade amplitude and target eccentricity in each group. Same participants and format as in Figure 3.

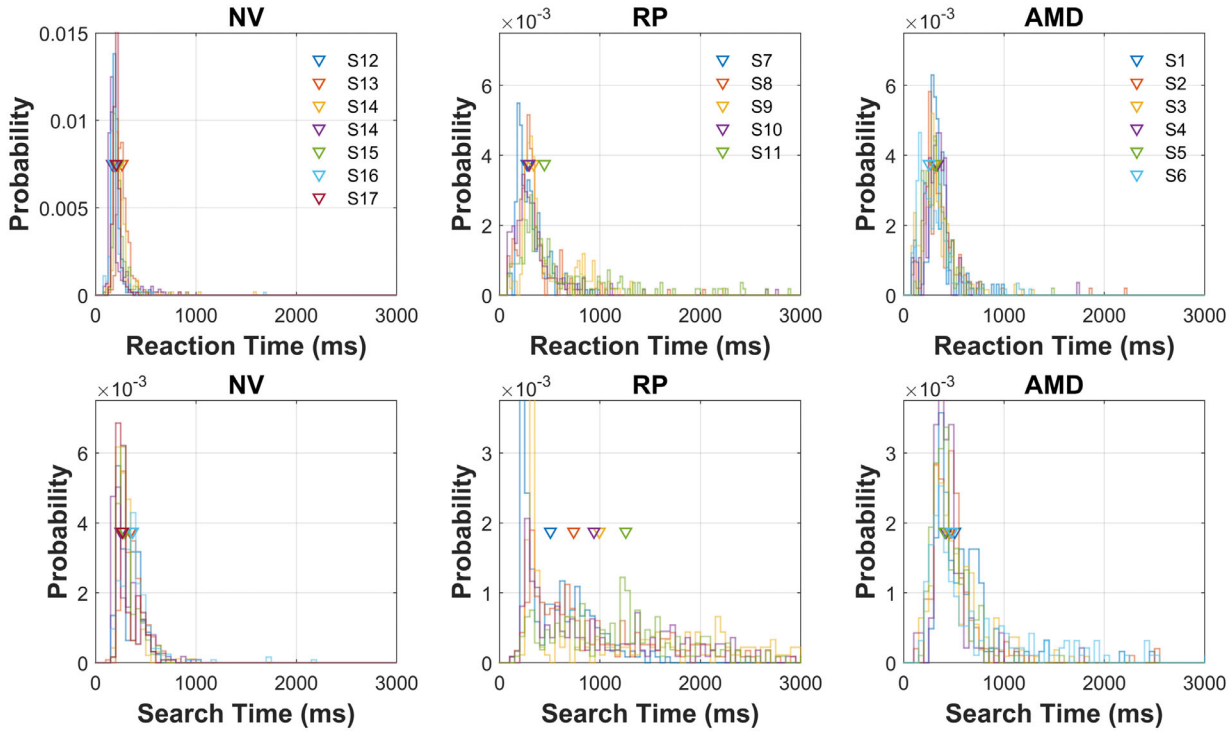

Figure 6. Reaction times and search times. Distribution of reaction times of primary saccades (**a**) and search times (**b**) in the odd trials (unpredictable target location). Primary saccades had to have a minimum latency of 80 ms and be directed away from the fixation point. Search time was measured from stimulus onset to the end point of best-landing saccade before the button press indicating that the subject had found the target. Colors represent different subjects, triangles the corresponding median reaction time or median search duration. Data are pooled across target locations. Note that the y-axis scales for NV differ from those for RP and AMD in the reaction time plots.

large saccades (>30 degrees), and the improved correlation for targets in the impaired peripheral field (black points). Supplementary Figure S2 shows these scatter plots for all individuals.

Even so, considering all largest goal-directed saccades in the odd trials (see boxplot in Fig. 5d), the correlations were significantly weaker (Wilcoxon rank sum test: $P < 0.005$) for both patients with RP (RP: median $\rho = 0.91$; range = 0.57–0.98) and patients with AMD (AMD: median $\rho = 0.97$; range = 0.92–0.98) compared to controls with NV (NV: median ρ =0.993; range = 0.955–0.996). Considering only the saccades in the patients' intact (see Fig. 5e) or impaired (see Fig. 5f) visual field, however, the correlations were not significantly different between the two patient groups (Wilcoxon rank sum tests: $P > 0.1$ and $P > 0.5$, respectively).

Reaction Times and Search Times

Besides reduced accuracy, the primary saccades of patients with RP and patients with AMD also had longer latencies than those in subjects with NV (Wilcoxon rank sum test, RP > NV: $P < 0.002$; AMD > NV: $P < 0.002$). The reaction time distributions shown in Figure 6a demonstrate this. Triangles indicate the median latency determined for each participant in the odd trials. Table 2 lists the group means and medians of these latency values. The latency impairments were present even for targets that appeared within the subjects' intact visual field (Wilcoxon rank sum test, RP_{intact} > NV: $P < 0.05$; AMD_{intact} > NV: $P < 0.002$), albeit less significantly in the RP group. The reaction times of primary saccades were not significantly different between the two patient groups (Wilcoxon rank sum tests, AMD ≠ RP: $P > 0.9$; $AMD_{intact} \neq RP_{intact}$: $P > 0.1$).

Table 2. Median Reaction Times

Group	*N*	Mean ± std (ms)	Median (ms)	Range (ms)
NV	7	207 ± 31	206	168–263
RP	5	328 ± 69	296	274–446
AMD	6	308 ± 29	319	254–337
RP_{intact}	5	272 ± 48	291	199–322
AMD_{intact}	6	308 ± 29	317	253–337

Listed are the mean ± standard, median, and range of the median reaction time of primary saccades for each of the three participant groups. Median latencies were determined from (odd) trials with targets appearing at unpredictable locations and pooled either across all target locations (rows 1–3) or including only those trials in which the target fell within the subject's intact visual field (rows 4-5).

Furthermore, both patients with RP and patients with AMD needed significantly more time to reach the target than subjects with NV (Wilcoxon rank sum test, RP > NV: $P < 0.002$; AMD > NV: $P < 0.001$). In addition, patients with RP had longer median search times than patients with AMD (Wilcoxon rank sum test, RP > AMD: $P < 0.005$). The search-time distributions depicted in the Figures 6d to 6f illustrate these findings. Table 3 quantifies the group means and medians of the search times.

Saccade Kinematics

The left-hand panels of Figure 7 show that the primary saccades of subjects with RP had, on average, longer

Table 3. Median Search Times

Group	*N*	Mean ± std (ms)	Median (ms)	Range (ms)
NV	7	299 ± 43	293	251–368
RP	5	887 ± 282	940	506–1257
AMD	6	455 ± 37	454	410–510

Listed are the mean ± standard, median, and range of the median search time for each of the three participant groups. Median search times were determined from (odd) trials with targets appearing at unpredictable locations and pooled across target locations.

durations (see Fig. 7a) and lower peak velocities (see Fig. 7b) than amplitude-matched primary saccades of subjects with NV. Here, the asterisks mark the amplitude bins for which these differences were statistically significant ($P < 0.05$) according to a Wilcoxon rank sum test on the subjects' median durations and peak velocities (Methods). The right-hand panels of Figure 7 (see Figs. 7c, 7d) show that a similar tendency was observed for subjects with AMD. However, the differences were typically much smaller. These plots include data from saccades with single-peaked and multi-peaked velocity profiles into the intact and affected visual field. The range of saccade amplitudes analyzed was restricted to amplitudes less than 22 degrees because the number of primary saccades with larger amplitudes was too limited in some of the patients. Note, that the boxplots in Figure 7 pool data across subjects. To illustrate the intersubject variability, Supplementary Figure S3 shows the main sequence of rightward and leftward saccades of the left and right eye in each individual subject.

To accommodate the intersubject variability in our analyses, we performed mixed effects regression (Methods). The results (solid lines) indicated that the patients with RP had, on average, significantly longer saccade durations than subjects with NV, and that these differences increased significantly with saccade amplitude ($P < 0.0001$; difference in slope: $\Delta a = 1.4$ ms/deg). In patients with AMD, saccade durations were significantly longer too ($P < 0.001$), but on average by only 2.8 milliseconds. The relation between peak velocity and saccade amplitude also differed significantly from subjects with NV. For both patients with RP and patients with AMD, the increase in peak velocity with saccade amplitude was significantly lower ($P < 0.005$; $1/\alpha = 107$ deg/s per

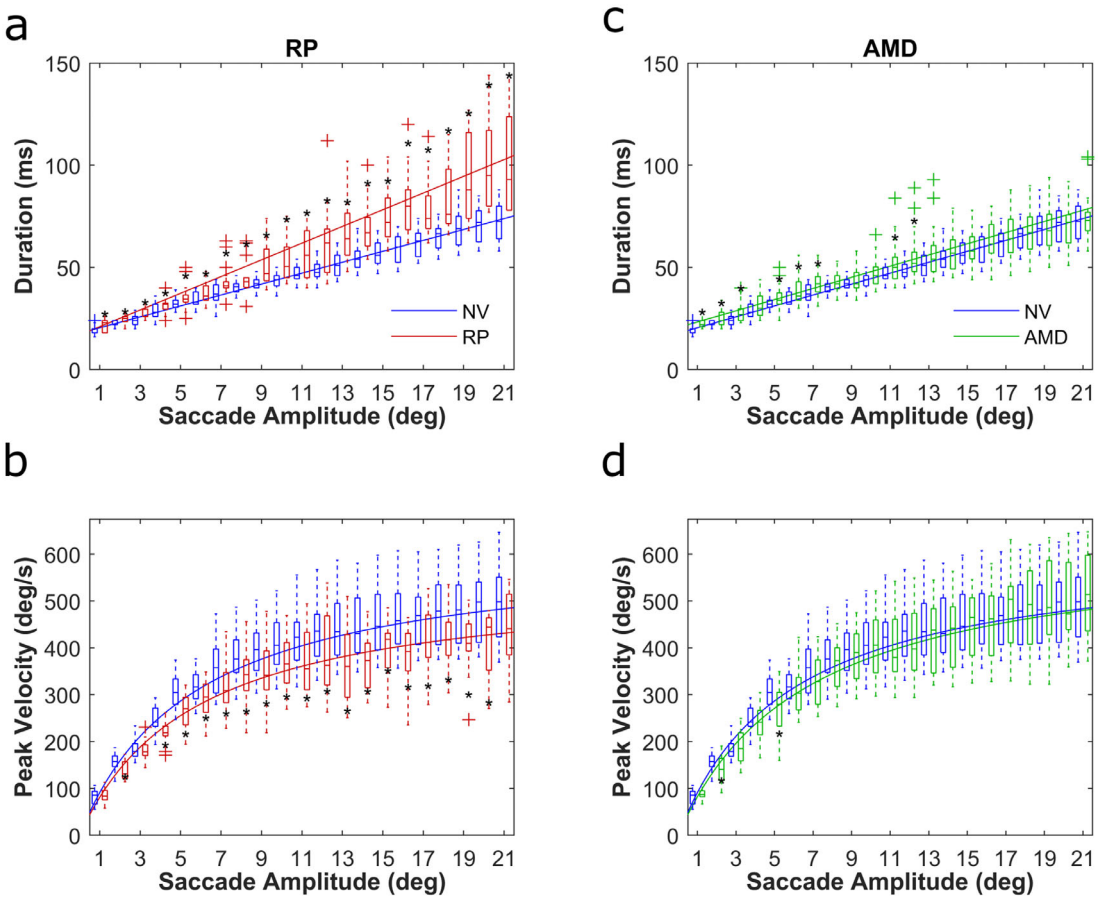

Figure 7. Main sequence of first saccades. Boxplots of median saccade duration and peak velocity versus saccade amplitude comparing the saccade kinematics in the RP (*red*) and AMD (*green*) patient group with the NV (*blue*) control group. Control data in **a, b** and **c, d** are duplicates. Median durations and peak velocities were determined in 2-degree-wide (overlapping) amplitude bins for each subject's eye and each saccade direction. Bin width was reduced to 1 degree for the first, 1-degree bin to better capture the steep increase in peak velocity in this amplitude range. Boxes are shifted to the left (NV) and right (RP/AMD) of the actual bin center for clarity. *Black asterisks*: Wilcoxon rank sum test, $P < 0.05$. Superimposed are mixed effects regression lines (marginal means). Data are from odd trials with targets at unpredictable, pseudo-random locations.

Investigative Ophthalmology & Visual Science

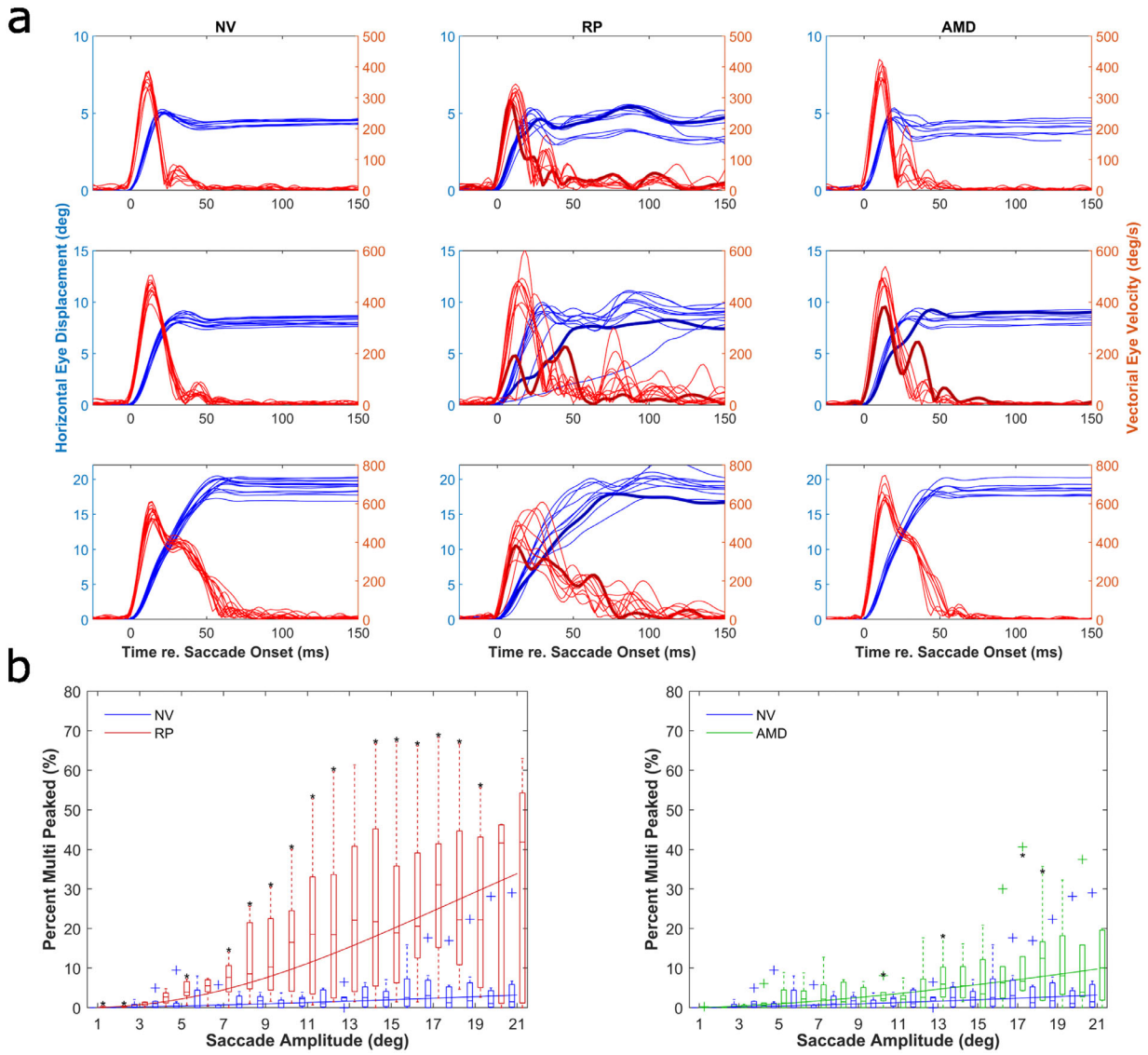

Figure 8. Saccades with multi-peaked velocity profiles. (**a**) Eye displacement (*blue*) and eye velocity (*red*) profiles of amplitude-matched saccades in three different amplitude ranges (4, 9, and 18 degrees). Data are from the same three participants as in Figure 2. Thick darker traces: selected examples of saccades with two or more velocity peaks. (**b**) Boxplots showing the percentage of saccades with multi-peaked velocity profiles as a function of saccade amplitude in the RP (*red*) and AMD (*green*) patient groups compared with the NV (*blue*) control group. *Black asterisks*: Wilcoxon rank sum test $P < 0.05$. *Solid curves*: Mixed effects regression lines (marginal means).

degree in the NV group versus $1/\alpha$ =95 deg/s per degree for the RP group, and $1/\alpha$ =95 deg/s per degree for the AMD group). This is best seen for small amplitudes, where the slope of the curve approach $1/\alpha$. In patients with RP, the saturation value of the curve also tends to be lower ($1/\beta$ = 616 deg/s for the NV group versus $1/\beta$ = 550 deg/s for the RP group), albeit not statistically significant (P = 0.07). Supplementary Tables S1 and S2 list the regression parameters of these analyses and corresponding statistics. A similar pattern of results was obtained for the even trials in which the subjects could anticipate the location of the target from the previous trial and a cuing triangle in the fixation point (data not shown).

As mentioned in the Methods, we noticed that some of the patients made many saccades with double or multi-peaked velocity profiles. To illustrate this, Figure 8a shows eye position (blue) and eye velocity (red) profiles for a number of saccades to three different target eccentricities. Thick darker traces are selected examples of saccades with two or more velocity peaks. To quantify this aberrant saccade behavior, the boxplots in Figure 8b show the percentage of saccades with multi-peaked velocity profiles in each amplitude bin. Note that the occurrence of such atypical saccades was most prominent in patients with RP and mostly for saccades that were larger than 7 to 9 degrees (i.e. saccades that were typically into their impaired peripheral visual field). A logistic mixed-effects model fitted to these data (solid lines)

Investigative Ophthalmology & Visual Science

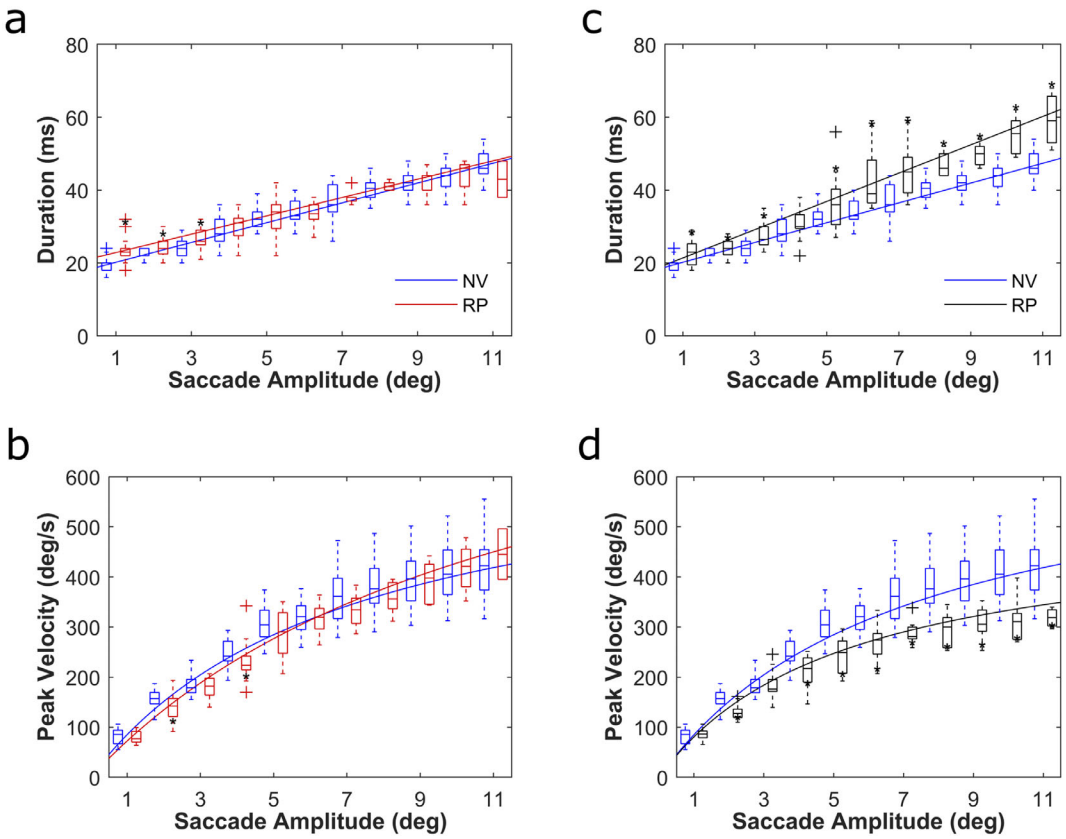

Figure 9. First saccades of patients with RP into their intact visual field. (**a, b**) Saccade and target both within the intact visual field. (**c, d**) Saccades of the same participants still directed to a location within the intact visual field but now for trials in which the target was located outside this region (e.g. on the contralateral side) and presumably not seen. Same format as Figure 7. Data are from saccades made in odd trials with targets at unpredictable, pseudo-random locations. Saccades with multi-peaked velocity profiles were excluded.

indicated that this amplitude effect was indeed statistically significant in the RP group ($P < 0.0001$; Supplementary Table S3).

Given the findings shown in Figure 8, we wondered if the longer durations and lower peak velocities in the patients only occurred in the saccades that had multi-peaked velocity profiles or whether the saccades with single-peaked velocity profiles were affected too. Mixed effects regression analyses of the data from Figure 7 indicated that even though the effects on saccade duration and peak velocity were attenuated, a qualitatively similar pattern of results was obtained when the analysis only included saccades with single-peaked velocity profiles (see Supplementary Figure S4, Supplementary Tables S4, S5).

Relation to Visual Field Defects

In subsequent analyses, we accounted for the subject-specific visual field deficits and examined whether the changes in kinematics of saccades with single-peaked velocity profiles were perhaps related to the location of the visual field defects.

Interestingly, we found, for patients with RP, that the durations and peak velocities of saccades to a location in their intact visual field were near normal when the saccades were to a target that was also in the intact visual field (Figs. 9a, 9b). This similarity did not result from the exclusion of saccades with multi-peaked velocity profiles that we applied here. The occurrence of such saccades was rare when the saccade and target were both in the intact visual field. If the target was in the impaired visual field, however, even single-peaked saccades into the intact visual field lasted longer and had lower peak velocities than saccades of the same amplitude in control subjects (Figs. 9c, 9d). As one might expect, these differences were larger if saccades with multi-peaked velocity profiles were included (not shown). Likewise, when both the target and the saccade were in the impaired visual field, saccade durations were significantly longer and peak velocities significantly lower than in subjects with NV, following the amplitude dependency shown in Figures 7a and 7b. Supplementary Tables S6 and S7 list the parameters of regression lines shown in Figure 9 together with their statistics.

In patients with AMD, the main sequence of saccades with single-peaked velocity profiles that were directed to targets in the intact visual field were, on average, significantly different from the main sequence of saccades in the control group with NV, but the differences were small (Figs. 10a, 10b). Saccades to a location within the intact visual field while the target was in a scotoma were very few in patients with AMD, and therefore not examined here. Because of the limited overlap of subjects' scotomas with the horizontal meridian (see Fig. 4), there were also not that many trials in which both the saccade and the target were within the scotoma, but there were enough trials for

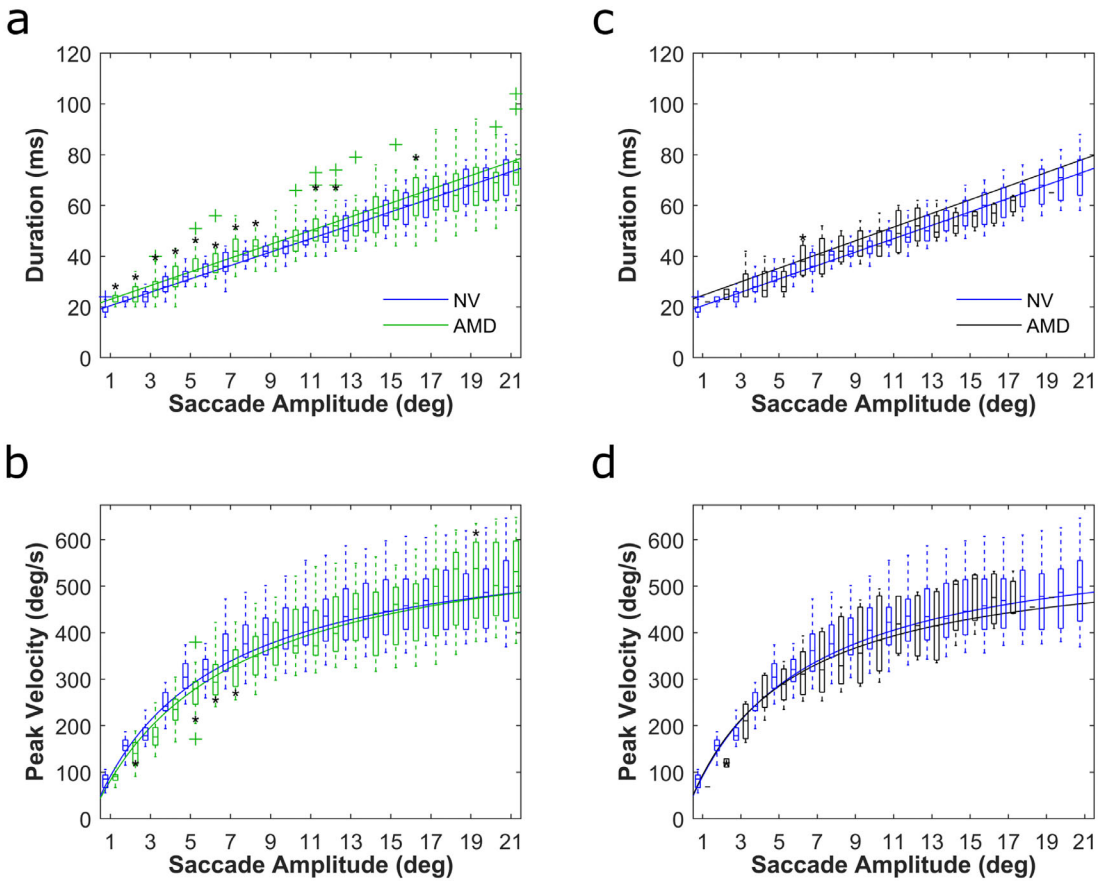

Figure 10. First saccades of patients with AMD into the intact and impaired visual field. (**a, b**) Saccade and target both within the intact visual field. (**c, d**) Saccade and target both within the subjects' scotoma. Same format as Figure 7. Data are from saccades made in odd trials with targets at unpredictable, pseudo-random locations. Saccades with multi-peaked velocity profiles were excluded.

a valid analysis. Even in this case, the duration and peak velocity of the saccades were remarkably similar to those of saccades made by controls with NV (Figs. 10c, 10d). Supplementary Tables S8 and S9 list the parameters of regression lines shown in Figure 10 together with their statistics.

Discussion

Our findings show that patients suffering from either foveal or peripheral vision loss not only have deficits in saccade reaction times and target localization behavior, but that the kinematics of the saccades are affected too. Especially in the patients with RP, who suffered from peripheral vision loss, saccades were generally slower, and the shape of the velocity profiles were often atypical. In the patients with AMD, who suffered from central vision loss, saccades were slower too, but the changes were far less dramatic than in the patients with RP.

Reaction Times and Search Times

To our knowledge, very few studies of eye movement behavior in patients with AMD and patients with RP have quantified the latency of primary saccades to single visual targets. Most previous studies have used visual search tasks instead.[24,25] As expected from these studies, the latencies of primary saccades were systematically longer in both patients with AMD and patients with RP compared to controls with NV (see Fig. 6, Table 2). In addition, we found that both patient groups needed more time to find the target (see Fig. 6, Table 3). The patients with RP in particular had the longest search times. Indeed, patients with RP often had to make a series of saccades to find the target, whereas subjects with NV or AMD would typically make a single one.

Saccade End Points

As one might expect from their peripheral field loss, patients with RP also had less accurate responses compared to patients with AMD (see Fig. 3). For targets appearing in their impaired visual field, the patients with RP essentially guessed whether the target would be to the left or right of the fixation point. Some of them adopted the strategy of making the first leftward or rightward saccade to a roughly fixed peripheral location whereas in others the saccade endpoints were more dispersed along the horizontal meridian. If the initial saccades did not bring the target within the intact visual field, often a large saccade in the opposite direction followed (see Fig. 5). The fact that the participants knew that stimuli were only presented on the horizontal meridian partly explains this strategy, and could differ, of course, if targets are presented throughout the visual field. We chose to restrict our stimuli to the horizontal meridian, however, because for each participant, we wanted to obtain a robust estimate of the main sequence and devia-

Investigative Ophthalmology & Visual Science

tions thereof in the absence of complicating factors, such as component stretching in oblique saccades.[34] This required a sufficient number of trial repetitions within each recording session.

In patients with AMD, the localization of targets within their scotoma(s) was surprisingly good. A possible explanation for this is that the participating patients with AMD had incomplete loss of vision in the affected areas, because geographic atrophy is patchy and there are areas where some photoreceptors remain (as visualized clinically by OCT B-scan and autofluorescence), allowing them to see or at least detect the targets. In addition, it is possible that the targets, which had a diameter of 1 degree, still had some overlap with an intact region of the visual field in one or the other eye. Even so, these observations have implications for the development of eye movement-based perimetric approaches as an alternative to standard perimetry assessment of visual field defects.[35–37]

The localization behavior that we observed seems consistent with studies by Turano et al.[38,39] They found that patients with central field loss had fixation patterns similar to those with normal vision while walking to a target.[38] Patients with RP, on the other hand, fixated over a larger area in the environment and on different features than did persons with NV when walking an unfamiliar route.[39]

Saccade Kinematics

Subjects with RP as well as subjects with AMD all showed main-sequence behavior. That is, there was a regular relationship among the amplitude, duration, and peak velocity of their saccades. Particularly, saccade duration increased linearly with increases in saccade amplitude, whereas peak velocity showed a saturating nonlinearity as in controls with NV. This is consistent with previous reports.[26,28]

However, the parameters of the main sequence relations differed from controls with NV, especially in patients with RP (see Fig. 7). On average, patients with RP made slower saccades than controls with NV (see Figs. 7a, 7b). Luo et al.,[26] on the other hand, did not observe these differences. This apparent discrepancy may be explained by the fact that Luo et al., who tested patients with RP in a visual search task, relied on previously published control data rather than testing subjects with NV themselves under the same conditions. Our findings in the AMD group are consistent with those of Whittaker et al.,[28] who reported that saccade durations are longer and peak velocities are lower in patients without fovea compared to controls with NV. However, in our study, the average differences between the AMD group and the NV group were small (see Figs. 7c, 7d; Supplementary Fig. S3) compared to those reported by Whittaker et al. (their figures 5 and 6). This difference in effect size could be due to several factors, including location and size of the patients' scotomas, PRL eccentricity, fixation stability, clinical diagnosis (most patients in the Whittaker et al. study had fundus flavimaculatus, only two had atrophic AMD) or task differences. Whittaker et al.[28] used two different letters (E and C) as peripheral saccade target, which the subjects had to discriminate within 6 seconds after presentation. This task demand could have emphasized saccade accuracy more so than the point stimuli we have used, resulting in a bigger effect on saccade kinematics.

Unlike the patients with AMD, the patients with RP in our study also made large numbers of saccades with atypically long durations and two or more peaks in the velocity profiles (see Fig. 8). The occurrence of such saccades was most prominent for large saccades into the impaired peripheral visual field, and are reminiscent of the abnormal velocity profiles of saccades that are accompanied by eye-blinks.[40,41] Maybe the lower velocities and multiple peaks reflect an adaptation to help "find" the target during the movements (e.g. by reducing image blur and saccadic suppression perhaps). In any case, it was not the amplitude of the saccade that determined deviations from the normal main sequence. In patients with RP, saccades to targets that were probably seen by the subject, were practically normal (see Fig. 9, left-hand panel), whereas saccades of similar amplitude were significantly slower than normal if the subject did not see the targets (because they appeared in their impaired peripheral field) and had to guess their location (see Fig. 9, right-hand panel). The findings in Figure 9 thus support the conclusion that visual inputs play an important role in planning the kinematics of a saccade. Interestingly, these "blind" saccades were not only slow, but the ones with a single-peaked velocity profile fell on a different main sequence. This behavior is reminiscent of the behavior reported for memory-guided saccades and anti-saccades, which are both slower than visually guided saccades of the same amplitude but still exhibit main sequence behavior.[34,42,43]

In patients with AMD, saccades made to targets that fell within the subjects' scotoma(s), had surprisingly normal durations and peak velocities (see Fig. 10, right-hand panels). In patients with RP, by contrast, saccades made to targets within their impaired peripheral field were slow. We think that this apparent discrepancy between the two patient groups relates to the fact that the patients with AMD localized the targets that appeared within their scotoma(s) relatively well, which betrays that the participating patients with AMD were somehow able to see or at least detect the presence of those targets (see also discussion above). It would be of interest, therefore, that future studies examine the kinematics of saccades in patients with AMD with severe localization deficits for targets presented in their scotoma(s).

As outlined in the introduction, optimal control theories[4–6,13–15] suggest that the stereotyped main sequence relations of foveating saccade reflect an optimal trade-off between speed and accuracy. Therefore, we initially speculated that patients with AMD might exhibit greater than normal saccade velocities, because their impaired foveal vision would no longer necessitate the same level of accuracy. These patients could have afforded, at least in theory, to make faster saccades at the expense of reduced saccade accuracy. Despite finding reduced accuracies in both patient groups (see Fig. 3), we found no evidence of increases in saccade velocity in either patient group compared to controls. However, we cannot exclude that the main sequence relations in patients with AMD do vary with the stability and eccentricity of their PRL. Other factors influence the main sequence as well.[44,45] In normally sighted subjects, for instance, we have found that peak velocity decreases and duration increases systematically with increasing latency.[16] Both in patients with AMD and in patients with RP, primary saccades had longer latencies, which could in part explain why saccades were slower. In addition, there is evidence that saccade peak velocity also decreases with statistical decision confidence.[18] Thus, uncertainty about the target location could have affected the motor commands.

Investigative Ophthalmology & Visual Science

Strengths and Limitations

We ensured, by using a monocular calibration procedure and by recording the movements of both eyes simultaneously, that we could reliably estimate the location of the residual visual field of both the left and right eye on a sample-to-sample basis. In this way, we were able to determine, for each saccade, whether the target had appeared in an intact part of the visual field or not, and thus account for the heterogeneity of the visual field deficits. Binocular recordings are important because it cannot be guaranteed that subjects always make conjugate movements or that their vergence angle remains fixed. At least one of the participants showed signs of a mild, alternating strabismus,[46] which was not detected in the ophthalmic screening. In future studies, we will consider implementing a more detailed binocular vision assessment in the screening process.

Another strength of our study is the use of mixed-effects regression models to accommodate intersubject variability and account for the nested structure of the repeated measurements in each participant. Furthermore, unlike an earlier study reporting on the kinematics of saccades in patients with RP,[26] we included a control group of elderly participants with NV. We should mention, however, that the average age of the participants with AMD (75 ± 8 years) was higher than that of the participants with NV (63 ± 12 years) and those with RP (62 ± 15 years) due to the inclusion of two 84-year-old patients with AMD. A difference between the patient groups can be expected because late AMD tends to occur later in life than moderate RP, which can develop earlier. We considered including age as a covariate in our analyses of the saccade kinematics, but because the mean and median ages were not significantly different between the groups (t-tests, $P > 0.05$; Wilcoxon rank sum tests, $P > 0.09$), and because the inclusion of age as a covariate did not change the pattern of results, we decided to drop this variable from the analyses. A study by Abel et al.[47] suggests that saccade peak velocity and duration are indeed not affected by aging. Latency, however, did increase with age in that study (as has been reported in other aging studies; but see Hopf et al.,[48] who first screened their participants with an ophthalmic examination). Thus, it is possible that the reported latency difference between the NV group and the AMD group (see Table 2) is partly due to age differences as well, even though we could not confirm the effect of age on saccade latency in our control group (Pearson's r $= -0.38$; $P > 0.4$).

A limitation of our study is the small number of included participants. Some of the results that we obtained for the AMD group reflect the fact that the disease and its progression is variable between patients. In two out of six subjects with AMD, the location of the scotomas was such that we ended up with only a small number of trials in which the target appeared within the subjects' bilateral scotoma(s). In a third patient with AMD, we blocked vision of the left eye because she had a parafoveal scotoma, with good remaining central vision. Future studies might consider an adjustment of the target locations according to the location of the subjects' scotomas to increase these numbers. We decided to use a fixed set of target locations instead. We did not want the stimulus set to differ between participants because this could elicit different response strategies. For instance, David et al.[49] found in a free-viewing task that the saccade direction, amplitude, and peak velocity are altered between different simulated scotomas.

Another limitation of our study is that we do not know how long our patients with AMD have had deteriorated foveal vision. However, geographic atrophy develops slowly, and upon clinical examination, these participants already had significant atrophy and scotomas. The longer a patient has had central vision loss, the more time they will have had to develop a stable PRL, and the more likely they will be to have a stable fixation.[17] In amblyopia, a decrease in fixation stability is associated with an increase in saccade latency.[50,51] Thus, the longer latencies of the patients with AMD may partly relate also to their PRL and fixation stability, even though we could not confirm this in our dataset.

Last, the presence of post-saccadic oscillations, especially in patients with RP, complicated the accurate marking of saccade endings. Data from surgically implanted coils in monkeys with simultaneous recording from an EyeLink 1000[52] suggest that PSOs reflect an underdamped oscillation of the pupil relative to the eyeball as the eyeball comes to a halt. Although we systematically discarded the PSOs from our analysis, the applied detection algorithm essentially marked the saccade ends at the first overshoot peak. This may have caused an overestimation of the amplitudes of some of the saccades and possibly an underestimation of their durations. This in turn may have biased the main sequence relations to some extent. We think, however, that the differences in PSO amplitude between controls and patients with RP and the resulting distortions of the main sequence curves are far too small to account for the robust differences in their main sequence relations. As one can estimate for instance from Figure 7, the error in measuring the true saccade amplitude of, say a 13-degree saccade, would have to be 2 degrees or more to account for the observed differences in peak velocity. Additionally, we noted that patients with RP made significantly more saccades with aberrant, multi-peaked velocity profiles.

Conclusions

Bilateral defects of the central and peripheral part of the retina not only affect reaction times, search times, and number of saccades to reach the target, but they also have distinct effects on the main sequence of saccades. Although it is difficult to link the changes in saccade kinematics to an adaptation strategy of the brain to compensate optimally for the actual visual deficits, our findings do support the conclusion that the altered visual inputs play an important role in the planning of the kinematics of a saccade. Eye movement-based perimetric approaches might use the fact that the "blind" saccades tend to be slow, at least in patients with RP.

Acknowledgments

Supported by the European Union Program FP7-PEOPLE-2013-ITN "HealthPAC," grant 604063 - IDP, the RadboudUMC, and the EU Horizon 2020 program, ERC advanced Grant, "Orient," nr. 693400.

Disclosure: **L. Guadron**, (N); **S.A. Titchener**, (N); **C.J. Abbott**, (N); **L.N. Ayton**, (N); **J. van Opstal**, (N); **M.A. Petoe**, (N); **J. Goossens**, (N)

References

1. Bahill AT, Clark MR, Stark L. Dynamic overshoot in saccadic eye movements is caused by neurological control signal reversals. *Exp Neurol*. 1975;48:107–122.
2. Leigh RJ, Kennard C. Using saccades as a research tool in the clinical neurosciences. *Brain*. 2004;127:460–477.
3. Ramat S, Leigh RJ, Zee DS, Optican LM. What clinical disorders tell us about the neural control of saccadic eye movements. *Brain*. 2007;130:10–35.
4. Harris CM, Wolpert DM. Signal-Dependent Noise Determines Motor Planning. *Lett to Nat*. 1998;394:780–784.
5. Harris CM, Wolpert DM. The main sequence of saccades optimizes speed-accuracy trade-off. *Biol Cybern*. 2006;95:21–29.
6. Saeb S, Weber C, Triesch J. Learning the optimal control of coordinated eye and head movements. *PLoS Comput Biol*. 2011;7:e1002253.
7. van Opstal AJ, Goossens HHLM. Linear ensemble-coding in midbrain superior colliculus specifies the saccade kinematics. *Biol Cybern*. 2008;98:561–577.
8. Ross J, Morrone MC, Goldberg ME, Burr CD. Changes in visual perception at the time of saccades. *Trends Neurosci*. 2001;24:113–121.
9. Gómez C, Canals J, Torres B, Delgado-García JM. Analysis of the fluctuations in the interspike intervals of abducens nucleus neurons during ocular fixation in the alert cat. *Brain Res*. 1986;381:401–404.
10. Pastor AM, Torres B, Delgado-Garcia JM, Baker R. Discharge characteristics of medial rectus and abducens motoneurons in the goldfish. *J Neurophysiol*. 1991;66:2125–2140.
11. Hu X, Jiang H, Gu C, Li C, Sparks DL. Reliability of oculomotor command signals carried by individual neurons. *Proc Natl Acad Sci USA*. 2007;104:8137–8142.
12. Goossens HHLM, van Opstal AJ. Optimal control of saccades by spatial-temporal activity patterns in the monkey superior colliculus. *PLoS Comput Biol*. 2012;8:e1002508.
13. Kardamakis AA, Moschovakis AK. Optimal control of gaze shifts. *J Neurosci*. 2009;29:7723–7730.
14. Tanaka H, Krakauer JW, Qian N. An optimization principle for determining movement duration. *J Neurophysiol*. 2006;95:3875–3886.
15. van Beers RJ. Saccadic eye movements minimize the consequences of motor noise. *PLoS One*. 2008;3:e2070.
16. Guadron L, van Opstal AJ, Goossens J. Speed-accuracy tradeoffs influence the main sequence of saccadic eye movements. *Sci Rep*. 2022;12:1–14.
17. Verghese P, Vullings C, Shanidze N. Eye Movements in Macular Degeneration. *Annu Rev Vis Sci*. 2021;7:773–791.
18. Seideman JA, Stanford TR, Salinas E. Saccade metrics reflect decision-making dynamics during urgent choices. *Nat Commun*. 2018;9:2907.
19. Schuchard RA. Preferred retinal loci and macular scotoma characteristics in patients with age-related macular degeneration. *Can J Ophthalmol*. 2005;40:303–312.
20. Greenstein VC, et al. Preferred Retinal Locus in Macular Disease. *Retina*. 2008;28:1234–1240.
21. White JM, Bedell HE. The oculomotor reference in humans with bilateral macular disease. *Invest Ophthalmol Vis Sci*. 1990;31:1149–1161.
22. Cornelissen FW, Bruin KJ, Kooijman AC. The influence of artificial scotomas on eye movements during visual search. *Optom Vis Sci Off Publ Am Acad Optom*. 2005;82:27–35.
23. Geisler WS, Perry JS, Najemnik J. Visual search: the role of peripheral information measured using gaze-contingent displays. *J Vis*. 2006;6:858–873.
24. van der Stigchel S, Bethlehem RA, Klein BP, Berendschot TT, Nijboer TC, Dumoulin SO. Macular degeneration affects eye movement behavior during visual search. *Front Psychol*. 2013;4:1–9.
25. Wiecek E, Pasquale LR, Fiser J, Dakin S, Bex PJ. Effects of peripheral visual field loss on eye movements during visual search. *Front Psychol*. 2012;3:1–13.
26. Luo G, Vargas-Martin F, Peli E. The role of peripheral vision in saccade planning: learning from people with tunnel vision. *J Vis*. 2008;8:25.1–25.8.
27. Titchener SA, Ayton LN, Abbott CJ, et al. Head and gaze behavior in retinitis pigmentosa. *Investig Ophthalmol Vis Sci*. 2019;60:2263–2273.
28. Whittaker S, Cummings R, Swieson L. Saccade control without a fovea. *Vision Res*. 1991;31:2209–2218.
29. Ferris FL III, Wilkinson CP, Bird A, et al. Clinical classification of age-related macular degeneration. *Ophthalmology*. 2013;120:844–851.
30. Brainard DH. The Psychophysics Toolbox. *Spat Vis*. 1997;10:433–436.
31. Nyström M, Hooge I, Holmqvist K. Post-saccadic oscillations in eye movement data recorded with pupil-based eye trackers reflect motion of the pupil inside the iris. *Vision Res*. 2013;92:59–66.
32. Mack DJ, Belfanti S, Schwarz U. The effect of sampling rate and lowpass filters on saccades – A modeling approach. *Behav Res Methods*. 2017;49:2146–2162.
33. Vargas-Martin F, Peli E. Eye movements of patients with tunnel vision while walking. *Invest Ophthalmol Vis Sci*. 2006;47:5295–5302.
34. Smit AC, Van Opstal AJ, Van Gisbergen JAM. Component stretching in fast and slow oblique saccades in the human. *Exp Brain Res*. 1990;81:325–334.
35. Jones PR, Lindfield D, Crabb DP. Using an open-source tablet perimeter (Eyecatcher) as a rapid triage measure for glaucoma clinic waiting areas. *Br J Ophthalmol*. 2021;105:681–686.
36. Jamara RJ, Van De Velde F, Peli E. Scanning eye movements in homonymous hemianopia documented by scanning laser ophthalmoscope retinal perimetry. *Optom Vis Sci*. 2003;80:495–504.
37. Gestefeld B, Grillini A, Cornelisssen FW, Marsman JB. Using eye tracking to simplify screening for visual field defects and improve vision rehabilitation. *Eye Track Res Appl Symp*. 2018, https://doi.org/10.1145/3204493.3207414.
38. Turano KA, Geruschat DR, Baker FH. Fixation behavior while walking: Persons with central visual field loss. *Vision Res*. 2002;42:2635–2644.
39. Turano KA, Geruschat DR, Baker FH, Stahl JW, Shapiro MD. Direction of gaze while walking a simple route: Persons with normal vision and persons with retinitis pigmentosa. *Optom Vis Sci*. 2001;78:667–675.
40. Goossens HHLM, Van Opstal AJ. Differential effects of reflex blinks on saccade perturbations in humans. *J Neurophysiol*. 2010;103:1685–1695.
41. Goossens HH, Van Opstal AJ. Blink-perturbed saccades in monkey. II. Superior colliculus activity. *J Neurophysiol*. 2000;83:3430–3452.
42. White JM, Sparks DL, Stanford TR. Saccades to remembered target locations: an analysis of systematic and variable errors. *Vision Res*. 1994;34:79–92.
43. Amador N, Schlag-Rey M, Schlag J. Primate antisaccades. I. Behavioral characteristics. *J Neurophysiol*. 1998;80:1775–1786.
44. Reppert TR, Choi JES, Haith AM, Shadmehr R. Changes in saccade kinematics associated with the value and novelty of a stimulus. *Conf Inf Sci Syst CISS 2012*. 2012;46:1–5.

45. Xu-Wilson M, Zee DS, Shadmehr R. The intrinsic value of visual information affects saccade velocities. *Exp Brain Res*. 2009;196:475–481.
46. Melis BJM, Cruysberg JRM, Van Gisbergen JAM. Listing's plane dependence on alternating fixation in a strabismus patient. *Vision Res*. 1997;37:1355–1366.
47. Abel L, Troost B, Dell'Osso L. The effects of age on normal saccadic characteristics and their variability. *Vision Res*. 1983;23:33–37.
48. Hopf S, Liesenfeld M, Schmidtmann I, Ashayer S, Pitz S. Age dependent normative data of vertical and horizontal reflexive saccades. *PLoS One*. 2018;13:1–13.
49. David EJ, Lebranchu P, Da Silva MP, Le Callet P. Predicting artificial visual field losses: a gaze-based inference study. *J Vis*. 2019;19:1–27.
50. Schor C, Hallmark W. Slow control of eye position in strabismic amblyopia. *Investig Ophthalmol Vis Sci*. 1978;17:577–581.
51. McKee SP, Levi DM, Schor CM, Movshon JA. Saccadic latency in amblyopia. *J Vis*. 2016;16:1–15.
52. Kimmel DL, Mammo D, Newsome WT. Tracking the eye non-invasively: Simultaneous comparison of the scleral search coil and optical tracking techniques in the macaque monkey. *Front Behav Neurosci*. 2012;6:1–17.

Investigative Ophthalmology & Visual Science